Noncontact Monitoring of Blood Oxygen Saturation Using Camera and Dual-Wavelength Imaging System

Article *in* IEEE transactions on bio-medical engineering · September 2015

DOI: 10.1109/TBME.2015.2481896

8 authors, including:

Dangdang Shao
Arizona State University
17 PUBLICATIONS **319** CITATIONS
SEE PROFILE

Chenbin Liu
Chinese Academy of Medical Science (CAMS) Shenzhen Cancer Hospital
45 PUBLICATIONS **613** CITATIONS
SEE PROFILE

Rafael Iriya
Arizona State University
11 PUBLICATIONS **333** CITATIONS
SEE PROFILE

Hui Yu
Shanghai Jiao Tong University
51 PUBLICATIONS **1,262** CITATIONS
SEE PROFILE

Noncontact Monitoring of Blood Oxygen Saturation Using Camera and Dual-Wavelength Imaging System

Dangdang Shao, Chenbin Liu, Francis Tsow, Yuting Yang, Zijian Du, Rafael Iriya, Hui Yu, and Nongjian Tao*

***Abstract*—We present a noncontact method to monitor blood oxygen saturation (SpO_2). The method uses a CMOS camera with a trigger control to allow recording of photoplethysmography (PPG) signals alternatively at two particular wavelengths, and determines the SpO_2 from the measured ratios of the pulsatile to the nonpulsatile components of the PPG signals at these wavelengths. The signal-to-noise ratio (SNR) of the SpO_2 value depends on the choice of the wavelengths. We found that the combination of orange ($\lambda = 611\,\mathrm{nm}$) and near infrared ($\lambda = 880\,\mathrm{nm}$) provides the best SNR for the noncontact video-based detection method. This combination is different from that used in traditional contact-based SpO_2 measurement since the PPG signal strengths and camera quantum efficiencies at these wavelengths are more amenable to SpO_2 measurement using a noncontact method. We also conducted a small pilot study to validate the noncontact method over an SpO_2 range of 83%–98%. This study results are consistent with those measured using a reference contact SpO_2 device ($r = 0.936$, $p < 0.001$). The presented method is particularly suitable for tracking one's health and wellness at home under free-living conditions, and for those who cannot use traditional contact-based PPG devices.**

***Index Terms*—Oxygen saturation, photoplethysmography (PPG), physiological signal tracking, remote sensing.**

I. Introduction

OXYGEN saturation, along with heart rate, breathing rate, blood pressure, and body temperature, is a vital physiological parameter. It is a relative measure of the oxygen amount dissolved or carried in a given medium, such as blood. It indicates whether a person has sufficient supply of oxygen and reflects the health level of the cardiorespiratory system. Continuous monitoring of oxygen saturation level is important in detecting hypoxemia under many medical situations, including anesthesia, sleep apnea, and parturition. It is employed in intensive care, operating room, emergency care, neonatal care, sleep study, and veterinary care [1].

Mixed venous oxygen saturation (SvO_2), tissue oxygen saturation (StO_2), and arterial oxygen saturation (SaO_2) are a few major methods used for the determination of oxygen saturation levels in human body. SvO_2 is a measurement of the oxygen remaining in the blood after passing through the capillary bed, which indicates moment-to-moment variation between oxygen supply and demand [2]. It can be monitored using fiber-optic catheters. StO_2 provides an assessment of tissue perfusion and it can be measured by near infrared (NIR) spectroscopy. SaO_2 is a measurement of oxygen saturation in the arteries. An estimation of SaO_2 at peripheral capillary is called SpO_2, which is the primary focus of this paper. Unlike traditional SaO_2 measurement, which is normally conducted invasively via a blood test with a blood gas analyzer, SpO_2 can be measured by noninvasive methods. Monitoring SpO_2 provides a quick and convenient assessment of user's oxygenation status. The most widely used device for SpO_2 monitoring is pulse oximeter, which is often attached to the finger for measurement purpose. The hardware implementation of pulse oximetry includes two main components: 1) an illumination source usually composed of a dual-wavelength LED, and 2) a photodetector—typically a photodiode. SpO_2 values typically range from 95% to 100% in healthy individuals. Continuous low SpO_2 levels ($<90\%$) may indicate an oxygen delivery problem [3].

Recent technological advances have enabled measurements of some of the physiological signals in noncontact ways [4]–[6]. Remote SpO_2 detection provides people with a method to measure oxygen saturation noninvasively under normal daily setting. Absence of physical contact between the subject and the device allows for a more comfortable and less stressful measurement condition. The inaccurate SpO_2 readings caused by varied pressure applied from finger to the contact sensor can also be avoided [7], besides preventing skin irritation that can occur in some individuals, especially infants, during extended monitoring periods. Noncontact pulse oximetry also provides a suitable SpO_2 measurement alternative for individuals with finger injuries, or for those with poor peripheral perfusion or dark pigmentation on fingers, for whom traditional pulse oximetry may otherwise lead to inaccurate measurements [8].

In recent years, researcher has attempted different SpO_2 measurement approaches using noncontact methods. Humphreys *et al.* [9], [10] used a CMOS camera with LED arrays that emit two different wavelengths as the light source for noncontact pulse oximetry. Due to low frame rate and sensitivity to ambient light, the noise in the measured PPG signals was too large to obtain accurate SpO_2 values. Wieringa *et al.* [11] also used a CMOS camera, but with three different wavelengths to investigate the feasibility of an "SpO_2 camera." However, no SpO_2 results were presented due to poor SNR of the PPG signals. Kong *et al.* [12] used two CCD cameras, each mounted with a narrow bandpass filter to capture PPG signals at two different wavelengths (520 and 660 nm) in ambient lighting condition. The test only covered a narrow SpO_2 range (97%–99%). For

Manuscript received May 27, 2015; revised August 28, 2015; accepted September 15, 2015. Date of publication September 24, 2015; date of current version May 18, 2016. This work was supported in part by the National Science Foundation. *Asterisk indicates corresponding author.*

D. Shao, F. Tsow, Z. Du, R. Iriya, and H. Yu are with the Biodesign Institute, Arizona State University.

C. Liu and Y. Yang are with the Department of Chemistry and Chemical Engineering, State Key Lab Analytical Chemistry Life Science, Nanjing University.

*N. J. Tao is with the Biodesign Institute, Arizona State University, Tempe, AZ 85287-5801 USA (e-mail: njtao@asu.edu).

Color versions of one or more of the figures in this paper are available online at http://ieeexplore.ieee.org.

Digital Object Identifier 10.1109/TBME.2015.2481896

practical applications, such as clinical settings, it is necessary to be able to measure SpO_2 over a wider range (at least 80%–100%). Tarassenko *et al.* [13] and Bal *et al.* [14] used a camera to calculate SpO_2 based on the PPG information obtained from the RGB channels under ambient lighting condition. Other researchers have found that the PPG signals extracted from the red and blue channels were noisier than those extracted from the green channel [6], [15], [16]. Moreover, for digital cameras, each color channel (red, green, or blue) covers a band of optical spectrum [17] with a width of $\sim 100\,\mathrm{nm}$, which is different from the traditional pulse oximetry method that uses monochromatic light sources with wavelengths selected to maximize the detection sensitivity of oxygenated and deoxygenated hemoglobin in blood. Tsai *et al.* [18], [19] used a CCD camera with red and infrared LEDs to take still images of hand and analyzed SpO_2 by looking into the reflective intensity of the shallow skin tissue. These authors compared the SpO_2 results against partial pressure of oxygen values (PaO_2), instead of the standard pulse oximetry. Although they showed correlation between the results obtained using the two methods, a direct demonstration of SpO_2 measurement is still lacking.

This paper describes a new noncontact method which is based on video recording of the subject's face area to measure SpO_2. To the best of the authors' knowledge, this is the first demonstration of a low-cost video-based method with high temporal resolution and signal-to-noise ratio to accurately monitor wide range of SpO_2 without any physical contact between the subject and the device. The contributions of this study include: 1) development of a hardware system with video capture and illumination synchronization control, 2) identification of optimized light sources to achieve accurate PPG and SpO_2 detection when using noncontact method, 3) validation of method over a wide clinically relevant range of SpO_2 via a pilot study of subjects, and 4) addition of SpO_2 tracking to our previously reported noncontact physiological monitoring platform, which can detect heart rate, breathing pattern, and pulse transit time [4].

II. Methods

A. SpO_2 Measurement Using a Dual-Wavelength Imaging System

SpO_2 is the percentage of oxygenated hemoglobin at peripheral capillary and can be expressed by the following equation:

$$\mathrm{SpO_2} = \frac{[\mathrm{HbO_2}]}{[\mathrm{HbO_2}] + [\mathrm{Hb}]} \times 100\%. \tag{1}$$

where $[HbO_2]$ is the concentration of oxygenated hemoglobin and [Hb] is the concentration of deoxygenated hemoglobin.

Traditional pulse oximetry measures SpO_2 based on the differential absorption of light by HbO_2 and Hb at two wavelengths. Depending upon the optical absorption spectrum of HbO_2 and Hb shown in Fig. 1, it is possible to select two wavelengths λ_1 and λ_2 such that absorbance by HbO_2 is more at λ_2 than at λ_1, while the absorbance by Hb is more at λ_1 than at λ_2.

The Beer–Lambert law—widely used to determine a solution's concentration by optical transmittance measurement—states that light absorption by a substance in a solution is

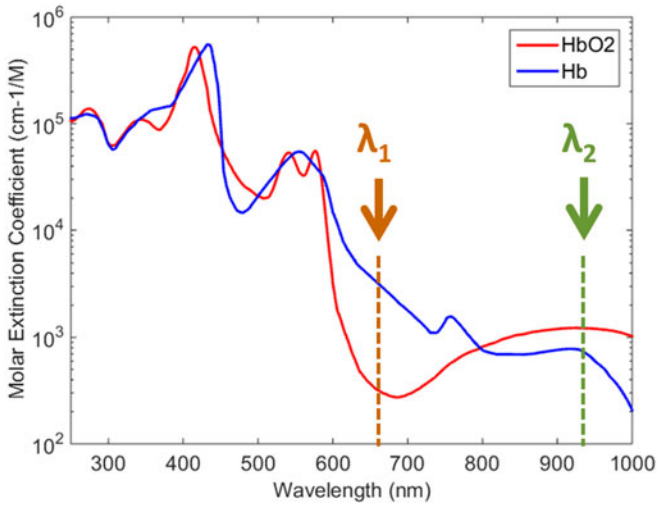

Fig. 1. Absorption spectra of HbO_2 and Hb (extinction coefficients from [20] with permission).

proportional to its concentration [21]. Pulse oximetry assumes that the pulsatile component (ac) of optical absorption originates from the pulsatile arterial blood, and the nonpulsatile component (dc) contains contributions from nonpulsatile arterial blood, venous blood, and other tissues. The pulsatile signals (ac) can be normalized by the nonpulsatile signals (dc) at λ_1 and λ_2 to give the pulsatile absorbance rates as follows:

$$R_{\lambda 1} = \frac{\mathrm{AC}_{\lambda_1}}{\mathrm{DC}_{\lambda 1}} \tag{2}$$

$$R_{\lambda_2} = \frac{\mathrm{AC}_{\lambda_2}}{\mathrm{DC}_{\lambda_2}}. \tag{3}$$

The ratio of absorbance at two wavelengths is defined as ratio of ratios RR

$$\mathrm{RR} = \frac{R_{\lambda_1}}{R_{\lambda_2}} = \frac{\mathrm{AC}_{\lambda_1}/\mathrm{DC}_{\lambda_1}}{\mathrm{AC}_{\lambda_2}/\mathrm{DC}_{\lambda_2}}. \tag{4}$$

RR can be regarded as nearly linear with respect to SpO_2 [12], [14], [22]:

$$\mathrm{SpO_2} = k \times \mathrm{RR} + b \tag{5}$$

where k and b are linear equation coefficients. Thus, SpO_2 value can be obtained by measuring RR. This dual-wavelength ratio method provides an easy way to determine SpO_2, and the result is independent of both light path length and concentration of blood constituents that absorb light.

Our SpO_2 detection is based on optical principles same to the traditional pulse oximetry. A key difference is our ability to track SpO_2 change using a noncontact method based on the reflected light. Further details of this method are provided in Section III-C.

B. Light Source Selection

As mentioned earlier, SpO_2 detection using the RR value requires employing at least two wavelengths. For accurate measurement, it is preferable that 1) the measured PPG signals have

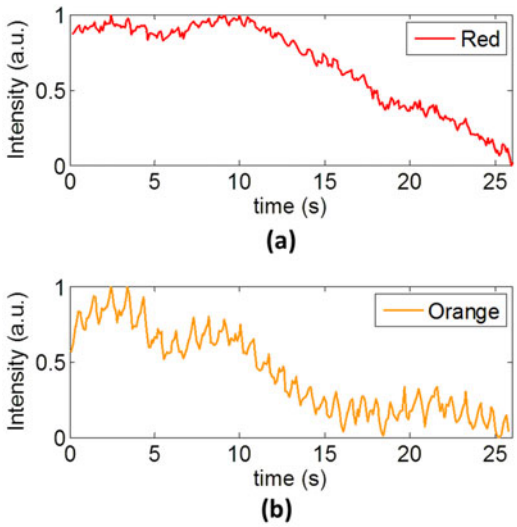

Fig. 2. PPG signals measured simultaneously using the camera with red ($\lambda = 660\,\mathrm{nm}$) and orange ($\lambda = 611\,\mathrm{nm}$) LEDs.

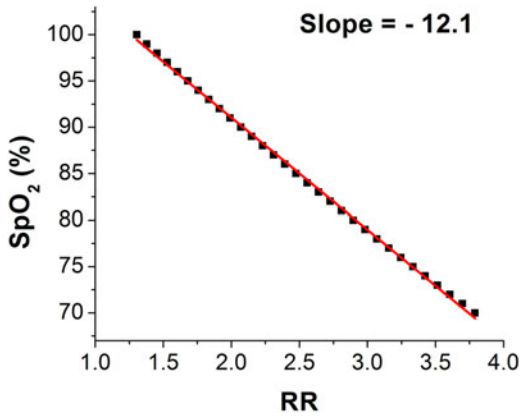

Fig. 3. Relationship between SpO_2 and RR (with wavelengths at 610 and 880 nm) based on (6) using extinction coefficients from [20]. The red line is a linear fit.

high SNR at both wavelengths, and 2) optical absorption associated with HbO_2 is opposite to that associated with Hb, and the differences between them are large at the two wavelengths, as shown in Fig. 1.

The traditional contact-based pulse oximetry uses a dual-wavelength LED at red ($\lambda = 660\,\mathrm{nm}$) and near infrared ($\lambda = 940\,\mathrm{nm}$) wavelengths as light source, and a photodiode as light detector. For transmission-mode pulse oximetry, the LED and photodiode are placed at either sides of the tissue (e.g., finger or earlobe), and for reflection-mode pulse oximetry, the LED and photodiode are positioned on the same side of the tissue. As per Fig. 1, the red light at 660 nm is absorbed more by Hb than by HbO_2, while the NIR light at 940 nm is absorbed more by HbO_2 than by Hb. The 660 and 940 nm wavelength combination produces high-quality data for the contact pulse oximetry, but it is not suitable for the presented noncontact method.

We observed that the use of red LED at 660 nm for the noncontact method results in poor PPG signal. To find a suitable replacement for the 660-nm LED, we evaluated the noncontact PPG signals at various wavelengths, ranging from 470 to 940 nm, and observed that the best PPG signal is obtained when green light is used, which is consistent with the literature [6], [15], [16]. However, the optical absorption difference between HbO_2 and Hb at green is small (see Fig. 1); thereby, making green unsuitable for SpO_2 measurement. We ruled out blue because its optical absorption is similar to NIR with high HbO_2 absorbance and low Hb absorbance despite the fact that its use produces good-quality PPG signal [23]. We determined orange ($\lambda = 590$ to $635\,\mathrm{nm}$) to be the most suitable substitute to red for our application because its optical absorption property fulfils the specified criteria—high Hb and low HbO_2 absorbance—and due to the superior PPG signals (shown in Fig. 2) measured via the noncontact method when using orange LED, as compared to red LED.

We also examined the suitability of the 940-nm LED—used in conventional contact pulse oximetry—for our imaging system, and found the PPG signal obtained using it to be unsatisfactory due to low SNR. The primary reason for this was the low quantum efficiency of the CMOS imager at 940 nm. NIR at wavelength 880 nm was found to provide better quality PPG signal obtained using the camera sensor. Moreover, 880 and 940 nm have similar optical absorptions by HbO_2 and Hb. These two reasons prompted the use of 880-nm LED, instead of 940-nm LED, in conjunction with the 610-nm orange LED for the presented method.

Performance of the 610-nm orange and 880-nm NIR combination was examined with a simulation of the dependence of RR on SpO_2 from 70% to 100%. The simulation was based on the Beer–Lambert law and the assumption that absorption of light in blood is only related to HbO_2 and Hb, which lead to the following RR equation:

$$\mathrm{RR} = \frac{s \times \varepsilon_{\mathrm{HbO_2}\_\lambda_1} + (1-s) \times \varepsilon_{\mathrm{Hb}\_\lambda_1}}{s \times \varepsilon_{\mathrm{HbO_2}\_\lambda_2} + (1-s) \times \varepsilon_{\mathrm{Hb}\_\lambda_2}} \tag{6}$$

where s is the oxygen saturation (SpO_2), and $\varepsilon_{\mathrm{HbO_2}\_\lambda_i}$ and $\varepsilon_{\mathrm{Hb}\_\lambda_i}$ are the extinction coefficients of HbO_2 and Hb at the two wavelengths [21]. The simulation result, as shown in Fig. 3, indicates that SpO_2 is linearly proportional to RR ($R^2 \sim 1$) with a maximum error $<0.6\%$ over a broad range (70%–100%), and can be approximated by (5). The linear relationship is consistent with other studies [12], [14], [22]. Coefficient k in (5) can be estimated from the linear fit curve slope, which is -12.1, as shown in Fig. 3.

Similar simulations with different wavelength combinations were carried out to determine the best wavelength combination for accurate SpO_2 measurement (see Fig. 4). For easy comparison of results at different wavelength combinations, each plot was normalized by the corresponding RR value at 100% SpO_2. The steeper the curve, the more sensitive a combination is to SpO_2 change. The red/NIR combination, which is widely used in the traditional pulse oximetry, shows the steepest curve. When SpO_2 drops from 100% to 70%, RR changes by 319%, indicating that this combination is most sensitive to SpO_2 change. How-

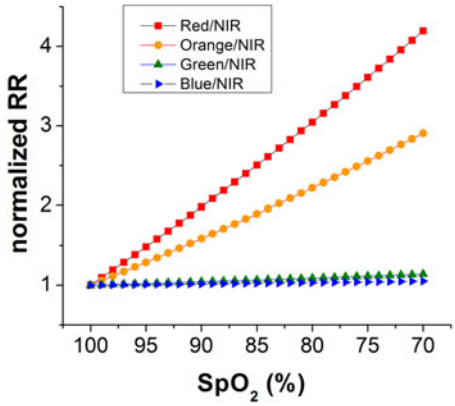

Fig. 4. Simulated plots of normalized RR versus SpO_2 based on four different wavelength combinations. (1) Red ($\lambda = 660\,\mathrm{nm}$) and NIR ($\lambda = 880\,\mathrm{nm}$). (2) Orange ($\lambda = 610\,\mathrm{nm}$) and NIR ($\lambda = 880\,\mathrm{nm}$). (3) Green ($\lambda = 528\,\mathrm{nm}$) and NIR ($\lambda = 880\,\mathrm{nm}$). (4) Blue ($\lambda = 470\,\mathrm{nm}$) and NIR ($\lambda = 880\,\mathrm{nm}$). The extinction coefficients used are from [20].

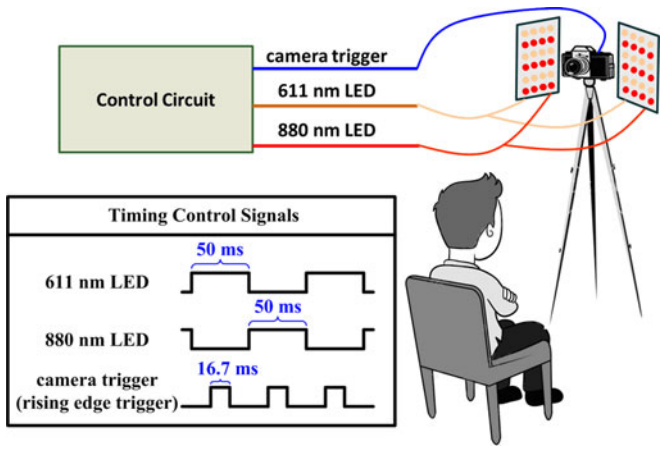

Fig. 5. Experimental setup and control signals.

ever, for the green/NIR and blue/NIR combinations, RR changes by only 14% and 5%, respectively, indicating their unsuitability to detect SpO_2 changes. The orange/NIR combination shows a change of RR by 190%. Although it is not as good as the red/NIR combination, it is the best choice for noncontact SpO_2 tracking when the SNRs of the PPG signals are considered.

C. Hardware Implementation

The experimental setup is shown in Fig. 5. A PixeLINK monochromatic camera PL-B741EU with a Fujinon HF16HA-1B 16-mm f/1.4 fixed focal lens was used to record the videos. The illumination system consisted of two identical LED arrays placed symmetrically on the left and right sides of the camera. Each array included alternating rows of NIR (QED223, Fairchild Semiconductor) and orange (SLI-570DT3F, Rohm Semiconductor) LEDs. A microcontroller (Texas Instruments MSP430F5348) was used to generate LED and camera trigger signals to switch the NIR and orange LEDs on and off alternatively so as to capture an image every 50 ms at the camera's trigger signal rising edge when either the NIR or the orange

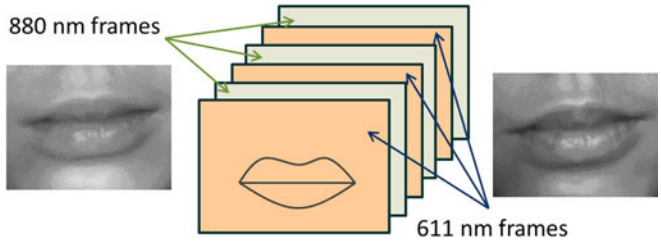

Fig. 6. Image sequence acquisition with two different wavelengths.

LEDs were on. The camera was triggered 20 times/s, so for each wavelength, the corresponding frame rate was 10 frames/s. All videos were taken indoors without ambient lights to avoid the noise.

D. Experiment Design

The subjects were asked to sit still approximately 30 cm from the camera and LED arrays. As long as clear focus and proper size were guaranteed for the region of interest (ROI), the distance did not affect the signal much, which was partially due to ac/dc normalization. A blindfold was used for comfort and eye protection. Each experiment lasted 5 min. As mentioned earlier, the normal SpO_2 range is 95%–100% in healthy people. To validate the presented method for low SpO_2 ($<$90%), we asked the subjects to hold their breath until they felt uncomfortable in order for their blood to reach low oxygen saturation level—a technique also used by other researchers [12], [22]. There is no known risk associated with holding breath for 0.5–1.5 min in healthy people. To produce a noticeable drop in SpO_2, the subjects must hold their breath for at least 30 s. Notwithstanding this equal time duration, the SpO_2 drop observed varied from one individual to another because of the varying lung capacity and hemoglobin oxygenation efficiency. We also noticed that after holding breath for 1 min, SpO_2 dropped below 90% in some subjects while in others, the drop was much smaller.

The subjects were asked to breathe normally for the first 2 min, during which the SpO_2 value was stable due to the sufficient oxygen supply. After this initial 2-min period, each subject was asked to hold breath as long as possible to produce an SpO_2 drop. When the subject resumed breathing, SpO_2 recovered to the same level as that before holding breath, usually within a few seconds.

SpO_2 measurements were also carried out simultaneously using a commercial contact pulse oximeter (Homedics PX-100) for comparison. The commercial device provided a reading nearly every 10 s.

E. Data Processing

Our previous study [4] has shown that the area around the lips provides a suitable region for good PPG signal measurement. For this reason, an area of 160×120 pixels around the lip was selected as the ROI. After capturing the videos, the ROI was analyzed using the following procedure. The acquired images were sorted into two groups, viz., NIR and orange as shown in Fig. 6, based on the wavelength at which they were captured.

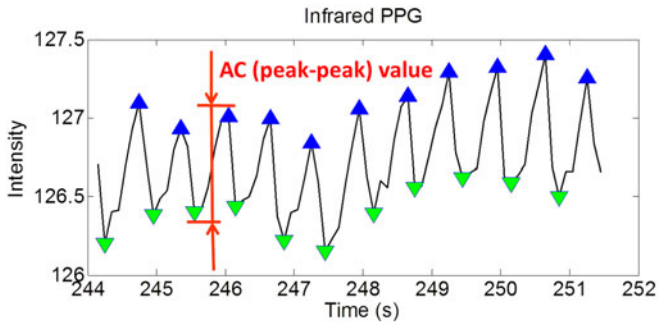

Fig. 7. AC value obtained from PPG signal.

In each group, the image intensity was averaged over all the ROI pixels in every frame to obtain the PPG signal at the corresponding wavelength. We divided each of the two PPG signals equally into 10-s subsets to provide SpO_2 data with a time resolution similar to the commercial contact pulse oximeter. For each of these subsets, the ac and the dc components of the PPG signal were obtained using the average peak-to-peak (see Fig. 7) and mean values, respectively. Fast Fourier transformation (FFT) can also be used to extract the PPG signal ac component [24]–[29], but it works well only when the heart rate remains constant, and yields inaccurate results when heart rate variability is high. The RR values were determined from (4) by using the measured ac and the dc PPG signal components. To extract SpO_2 from RR, we used (5), where k was determined from the slope of the plot shown in Fig. 3, and the intercept b was determined from the baseline SpO_2 level and corresponding average RR value obtained during the initial 2 min of each test.

III. Results

A. Validation of the Wavelength Selection

We first validated the detection of noncontact PPG signals at 611 and 880 nm. We recorded PPG signals at the two wavelengths simultaneously, both showing heart beating clearly as plotted in Fig. 8. AC/DC normalization was used for compensating the difference in image intensities at the two wavelengths [see (2), (3)]. FFT spectra of the simultaneously recorded PPGs at the two wavelengths show pronounced peaks at 1.5 Hz, which correspond to the heart rate.

When SpO_2 drops, HbO_2 concentration decreases, and Hb concentration increases. In this case, we expect that more orange light and less NIR light will be absorbed. Consequently, the reflectance of orange light will drop and that of the NIR light will increase. When SpO_2 increases, opposite changes in the reflectance are expected. Fig. 9 shows that the average intensity at 880 nm increased when the subject held breath (SpO_2 dropped) and decreased after the subject resumed breathing (SpO_2 increased). It also shows an opposite trend at 611 nm. These observations are consistent with the optical absorption properties of HbO_2 and Hb at 611 and 880 nm.

B. SpO_2 Measurement

Fig. 10 shows two sets of measurements performed for validation purpose, wherein SpO_2 values were obtained using the presented method (black curve) and were compared against those obtained using the reference device (red curve) every 10 s over a 5-min measurement duration. The stable SpO_2 value at 98% corresponds to the normal breathing period of 2 min and the evident reduction corresponds to the time period for which breath is held. The SpO_2 value restoration corresponds to the resumption of normal breathing. A delay ($\sim$10 s) in the reading of the reference pulse oximeter was corrected for comparison with the noncontact SpO_2 detection. The comparison shown in Fig. 10 indicates that the SpO_2 measured using the noncontact method is consistent with that measured using the contact-based reference method.

C. Small-Scale Pilot Study

To demonstrate the robustness of our noncontact method to monitor SpO_2, a small-scale pilot study was conducted and statistical analysis of the data was completed. Six subjects were enrolled in the Institutional Review Board study approved by Arizona State University (No. STUDY00002240). The subjects included different genders (three males, three females), ages (27.3 ± 2.8 years old, $\mathrm{mean} \pm \mathrm{SD}$), and skin colors. Informed consents were obtained from all the subjects following an approved protocol. None of the subjects had any known respiratory disease. We repeated the test as described in the last section on different subjects and compared the lowest SpO_2 values determined using the presented method and reference pulse oximetry. Fig. 11 shows a plot of the lowest SpO_2 values from 43 tests and linear least square regression. A good linear correlation ($R^2 = 0.87$) is found between the presented and reference methods over a wide range of oxygen saturation levels. Slope of the linear fitting curve is about 0.86, which is small than the ideal value of 1, with standard error of 0.05. The data are dispersed around the linear curve, which may be attributed to subject movement, and light scattering effects.

Bland–Altman plots were used to further evaluate the test results (see Fig. 12). The mean of the differences between the presented method and reference method is -0.07%. The interval for 95% limits of agreement between the two methods is from -2.65% to 2.51%, which is calculated by mean difference $\pm 1.96 \times$ standard deviation of the differences. The root-mean-square error is 1.3 and r is 0.936 ($p < 0.001$). Since $p < 0.05$ indicates a significant correlation between the two methods under comparison, we conclude that the observed correlation between our noncontact SpO_2 detection method and the traditional contact pulse oximetry is statistically significant.

IV. Discussion

The lowest SpO_2 observed during testing for this study was 83%. Lower SpO_2 values were difficult to achieve by holding breath in healthy individuals. A person with SpO_2 lower than 80% is considered to be in a state of hypoxia. Our method was validated for SpO_2 values ranging from 83%–100%, which

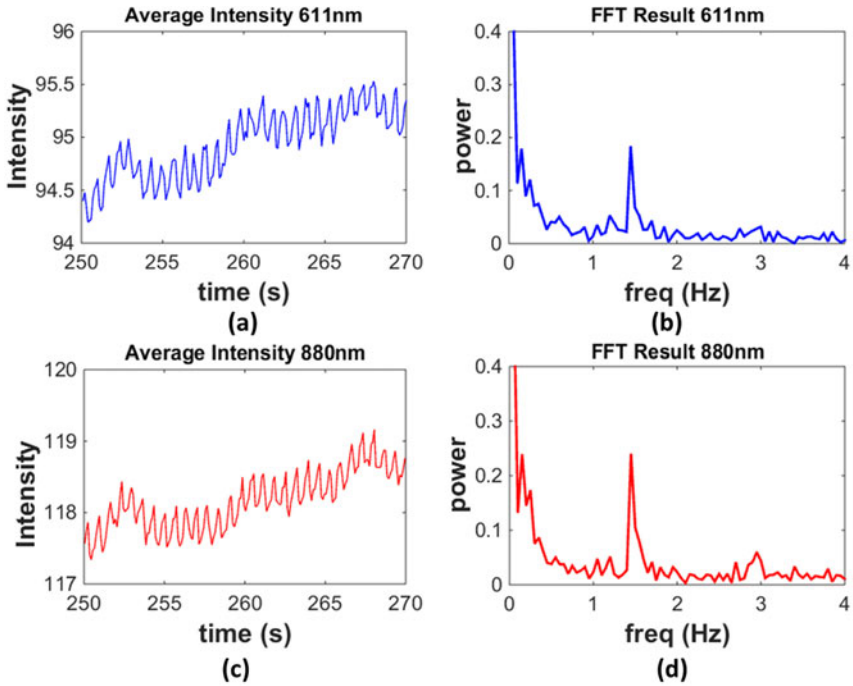

Fig. 8. PPG signals obtained at 611 and 880 nm (a), (c), and the corresponding FFT spectra (b), (d).

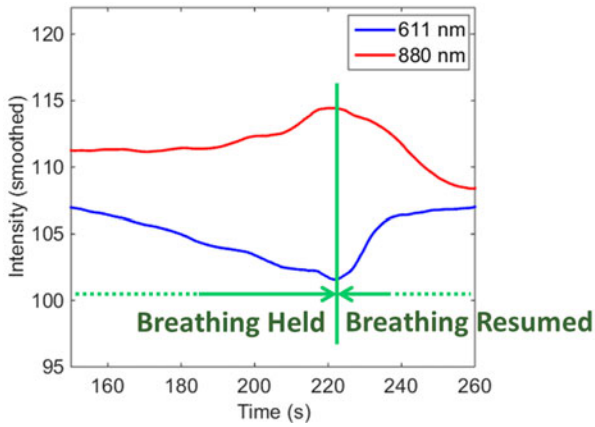

Fig. 9. Image intensity changes due to SpO_2 variation. Each PPG signal has been smoothed by a 100-point moving average filter.

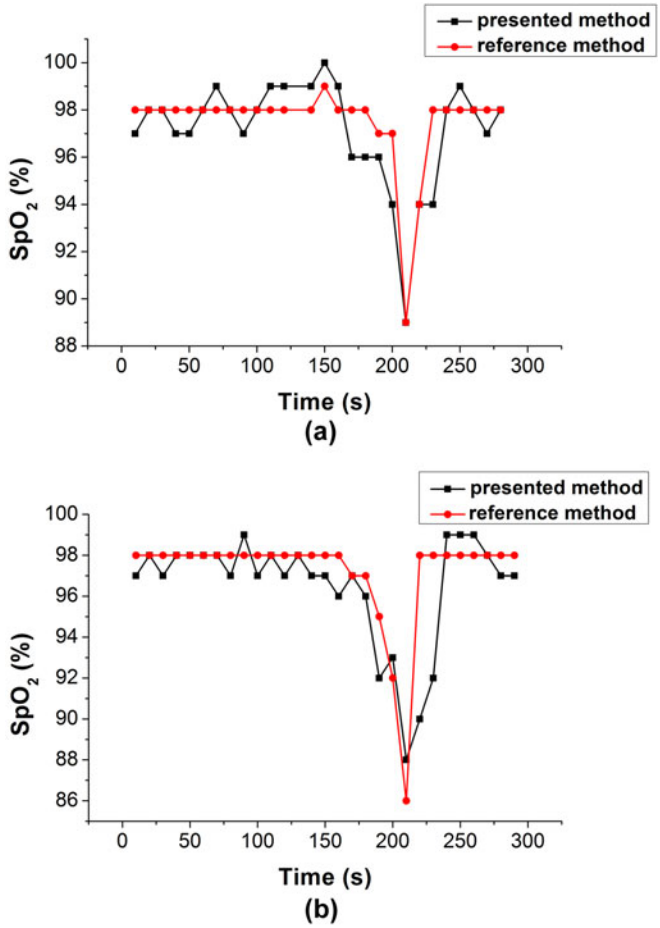

Fig. 10. (a), (b) SpO_2 measured using a pulse oximeter (reference method, red curve) and using the presented method (black curve).

is the normal oxygen saturation level range in most healthy individuals. Thus, the presented method can be used for daily SpO_2 monitoring.

Compared to the traditional contact pulse oximetry, noncontact pulse oximetry is considerably more challenging. This study demonstrated the feasibility of measuring SpO_2 accurately with a noncontact method, but there are several improvements that can be made in the future, some of which are discussed here. First, the camera used for PPG signal detection in this study has a sampling rate of 20 Hz, which is much lower than the 480-Hz sampling rate that the traditional pulse oximeter can typically reach [10]. Yet another related issue is the missing frames, which can range from 5%–10% of the total number of captured frames, due to the camera's hardware and software

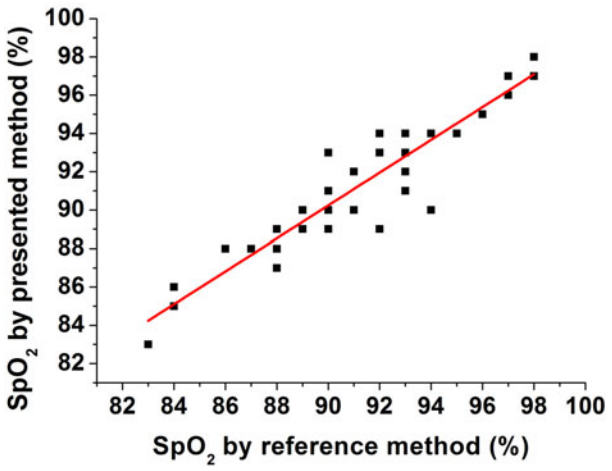

Fig. 11. Correlation between the lowest SpO_2 values obtained from the presented noncontact and reference contact methods. The red line is a linear fit.

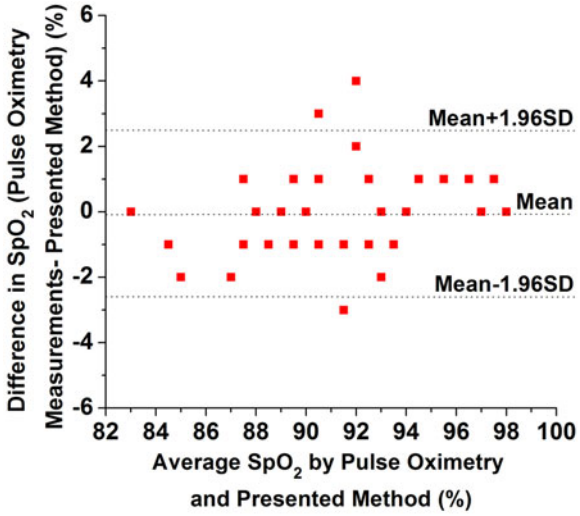

Fig. 12. Bland–Altman plot showing the difference between the SpO_2 values measured using the presented noncontact method and the commercial contact pulse oximetry versus the average values of the two methods.

limitations. Both of these issues can be addressed by using a higher quality imaging system. Second, although this paper's scope is limited to the validation of our noncontact method for SpO_2 tracking with subjects sitting relatively still on a chair, motion-tracking algorithms can be used in the future works to mitigate PPG signal deterioration arising from subject movements [30], [31] so as to improve the system's robustness and augment the extent of utilization. Finally, in this study, a commercial pulse oximeter was used as reference instead of arterial blood gas analysis—the gold standard for pulse oximetry development. The error of commercial pulse oximeter is about $\pm 2\%$–3% for normal SpO_2 (95%–100%) and can be as large as $\pm 8\%$ when SpO_2 drops to very low levels ($<80\%$) [32]. Replacing commercial pulse oximeter with blood gas analyzer (e.g., CO-oximeter) to perform *in vivo* calibration will improve the accuracy of the presented method. However, blood gas analysis is typically an invasive technique and requires special equipment usually only available in clinical settings—the lack of which during the development of the presented system limited our analysis to the use of a theoretical model such as (6), which is derived using the Beer–Lambert law. As stated earlier, the curve for RR and SpO_2 was approximated to be linear over the SpO_2 range of 70% to 100% when using (6) and the linear coefficient k was determined for it. Nevertheless, the Beer–Lambert law does not take into account the effects of light scattering at the skin surface when measuring PPG in reflective mode. Light scattering changes the optical path length, and, thus, affects the total apparent absorbance [32]. Building a more accurate optical model to incorporate the effects of light scattering is a difficult task. Therefore, other researchers adopt approaches that include development and application of advanced mathematical models [33], [34] or empirical correction schemes to better describe the relationship between RR and SpO_2. These correction methods will be implemented in the future works to further improve the presented method.

V. Conclusion

We have demonstrated a video-based noncontact method to monitor SpO_2 that was implemented using a CMOS camera to record PPG signals with light source alternating at two different 611 and 880 nm wavelengths. We found that the selection of light source was critical for accurate SpO_2 tracking with the noncontact method, and ac/dc component analysis of the PPG signals was more relevant than direct image intensity analysis. The results measured using the method presented here were consistent with those obtained using the reference device over a wide SpO_2 range. We also carried out a small-scale pilot study involving multiple subjects to validate the method. Our study could potentially offer a low-cost solution for people who wish to track their SpO_2 along with other vital physiological parameters under normal living conditions without wearing any devices. Future works will include using higher quality imaging system for faster frame rate and minimized frame loss, using gold standard arterial blood test analysis to calibrate the presented method, including the influence of light scattering in our model, and recruiting a large cohort of study subjects having various health conditions to further validate the usability of the noncontact SpO_2 detection method.

References

[1] M. Tavakoli *et al.*, "An ultra-low-power pulse oximeter implemented with an energy-efficient transimpedance amplifier," *IEEE Trans. Biomed. Circuits Syst.*, vol. 4, no. 1, pp. 27–38, Jan. 2010.

[2] *Understanding Continuous Mixed Venous Oxygen Saturation (SvO_2) Monitoring With the Swan–Ganz Oximetry TD System*, Edwards Lifesciences LLC, Irvine, CA, USA, 2002, p. 1.

[3] *What Does SpO_2 Mean? What is the Normal Blood Oxygen Level?*" Withings, Issy-les-Moulineaux, France (2015). [Online]. Available: https://withings.zendesk.com/hc/en-us/articles/201494667-What-does-SpO_2-mean-What-is-the-normal-blood-oxygen-level-

[4] D. Shao *et al.*, "Noncontact monitoring breathing pattern, exhalation flow rate and pulse transit time," *IEEE Trans. Biomed. Eng.*, vol. 61, no. 11, pp. 2760–2767, Nov. 2014.

[5] M.-Z. Poh *et al.*, "Advancements in noncontact, multiparameter physiological measurements using a webcam," *IEEE Trans. Biomed. Eng.*, vol. 58, no. 1, pp. 7–11, Jan. 2011.

[6] W. Verkruysse *et al.*, "Remote plethysmographic imaging using ambient light," *Opt. Exp.*, vol. 16, no. 26, pp. 21434–21445, Dec. 2008.
[7] V. Kamat, "Pulse oximetry," *Indian J. Anaesth.*, vol. 46, no. 4, pp. 261–268, 2002.
[8] P. E. Bickler *et al.*, "Effects of skin pigmentation on pulse oximeter accuracy at low saturation," *Anesthesiology*, vol. 102, no. 4, pp. 715–719, 2005.
[9] K. Humphreys *et al.*, "A CMOS camera-based pulse oximetry imaging system," in *Proc. IEEE Eng. Med. Biol. Soc. Conf.*, Shanghai, China, 2005, vol. 4, pp. 3494–3497.
[10] K. Humphreys *et al.*, "Noncontact simultaneous dual wavelength photoplethysmography: A further step toward noncontact pulse oximetry," *Rev. Sci. Instrum.*, vol. 78, no. 4, p. 044304, 2007.
[11] F. P. Wieringa *et al.*, "Contactless multiple wavelength photoplethysmographic imaging: A first step toward 'SpO_2 camera' technology," *Ann. Biomed. Eng.*, vol. 33, no. 8, pp. 1034–1041, 2005.
[12] L. Kong *et al.*, "Non-contact detection of oxygen saturation based on visible light imaging device using ambient light," *Opt. Exp.*, vol. 21, no. 15, pp. 17464–17471, 2013.
[13] L. Tarassenko *et al.*, "Non-contact video-based vital sign monitoring using ambient light and auto-regressive models," *Physiol. Meas.*, vol. 35, no. 5, pp. 807–831, 2014.
[14] U. Bal, "Non-contact estimation of heart rate and oxygen saturation using ambient light," *Biomed. Opt. Exp.*, vol. 6, no. 1, pp. 86–97, Dec. 2014.
[15] U. S. Freitas, "Remote camera-based pulse oximetry," in *Proc. 6th Int. Conf. eHealth, Telemed., Social Med.*, Barcelona, Spain, 2014, pp. 59–63.
[16] J. Lee *et al.*, "Comparison between red, green and blue light reflection photoplethysmography for heart rate monitoring during motion," in *Proc. IEEE Eng. Med. Biol. Soc. Conf.*, 2013, pp. 1724–1727.
[17] J. Jiang *et al.*, "What is the space of spectral sensitivity functions for digital color cameras?" in *Proc. Workshop Appl. Comput. Vis.*, 2013, pp. 168–179.
[18] H.-Yi Tsai *et al.*, "A study on oxygen saturation images constructed from the skin tissue of human hand," in *Proc. IEEE Int. Instrum. Meas. Technol. Conf.*, Minneapolis, MN, USA, May 2013, pp. 58–62.
[19] H.-Y. Tsai *et al.*, "A noncontact skin oxygen-saturation imaging system for measuring human tissue oxygen saturation," *IEEE Trans. Instrum. Meas.*, vol. 63, no. 11, pp. 2620–2631, Nov. 2014.
[20] S. Prahl, *Optical Absorption of Hemoglobin*, Oregon Medical Laser Center, Portland, OR, USA (1998). [Online]. Available: http://omlc.org/spectra/hemoglobin/summary.html
[21] G. M. Azmal *et al.*, "Continuous measurement of oxygen saturation level using photoplethysmography signal," in *Proc. IEEE Int. Conf. Biomed. Pharmaceutical Eng.*, Singapore, 2006, pp. 504–507.
[22] C. G. Scully *et al.*, "Physiological parameter monitoring from optical recordings with a mobile phone," *IEEE Trans. Biomed. Eng.*, vol. 59, no. 2, pp. 303–306, Feb. 2012.
[23] L. F. C. Martinez *et al.*, "Optimal wavelength selection for noncontact reflection photoplethysmography," in *Proc. SPIE, 22nd Congr. Int. Commission Opt.*, vol. 8011, p. 801191 Nov. 2011.
[24] W. S. Johnston, "Development of a signal processing library for extraction of SpO_2, HR, HRV, and RR from photoplethysmographic waveforms," M.S. thesis, Dept. Biomed. Eng., Worcester Polytechnic Inst., Worcester, MN, USA, 2006.
[25] T. L. Rusch *et al.*, "Alternate pulse oximetry algorithms for SpO_2 computation," in *Proc. IEEE Eng. Med. Biol. Soc. Conf.*, Baltimore, MD, USA, Nov. 1994, vol. 2, pp. 848–849.
[26] J. E. Scharf *et al.*, "Pulse oximetry through spectral analysis," in *Proc. 12th Southern Biomed. Eng. Conf.*, New Orleans, LA, USA, Apr. 1993, pp. 227–229.
[27] J. E. Scharf and T. L. Rusch, "Optimization of portable pulse oximetry through Fourier analysis," in *Proc. 12th Southern Biomed. Eng. Conf.*, New Orleans, LA, USA, Apr. 1993, pp. 233–235.
[28] T. L. Rusch *et al.*, "Signal processing methods for pulse oximetry," *Comput. Biol. Med.*, vol. 26, no. 2, pp. 143–159, 1996.
[29] J. M. Kim *et al.*, "Signal processing using Fourier & wavelet transform for pulse oximetry," in *Proc. Conf. Lasers Electro-Opt.*, Chiba, Japan, 2001, vol. 2, pp. 310–311.
[30] Y. Sun *et al.*, "Motion-compensated noncontact imaging photoplethysmography to monitor cardiorespiratory status during exercise," *J. Biomed. Opt.*, vol. 16, no. 7, p. 077010, 2011.
[31] L. Feng *et al.*, "Motion-resistant remote imaging photoplethysmography based on the optical properties of skin," *IEEE Trans. Circuits Syst. Video Technol.*, vol. 25, no. 5, pp. 879–891, May 2015.
[32] J. G. Webster, *Design of Pulse Oximeters*. London, U.K.: Institute of Physics Publishing, 1997.
[33] I. Fine and A. Weinreb, "Multiple scattering effect in transmission pulse oximetry," *Med. Biol. Eng. Comput.*, vol. 33, no. 5, pp. 709–712, 1995.
[34] G. Zonios *et al.*, "Pulse oximetry theory and calibration for low saturations," *IEEE Trans. Biomed. Eng.*, vol. 51, no. 5, pp. 818–822, May 2004.

Authors' photographs and biographies not available at the time of publication.